Title
BOOTSTRAP CALCULATIONS OF nn SCATTERING USING THE MANDEL-STAM ITERATION

Author
Webber, Bryan R.

Publication Date
1970-10-01

Submitted to Physical Review

UCRL-20134
Preprint

c.2

BOOTSTRAP CALCULATIONS OF $\pi\pi$ SCATTERING USING THE MANDELSTAM ITERATION

Bryan R. Webber

October 15, 1970

AEC Contract No. W-7405-eng-48

LAWRENCE RADIATION LABORATORY
UNIVERSITY of CALIFORNIA BERKELEY

DISCLAIMER

BOOTSTRAP CALCULATIONS OF $\pi\pi$ SCATTERING USING THE MANDELSTAM ITERATION*

Bryan R. Webber

Lawrence Radiation Laboratory
University of California
Berkeley, California 94720

October 15, 1970

ABSTRACT

The results of some strip model calculations of $\pi\pi$ scattering are presented. In these calculations, unitarity is imposed by means of the Mandelstam iteration. This procedure has the advantage that the output trajectories and residues (including their imaginary parts) may be computed above as well as below threshold; this is at present not feasible in calculations using the N/D technique. First, a bootstrap calculation of the ρ trajectory is carried out, neglecting Pomeranchuk exchange. The extra requirement of self-consistency above threshold is very strict, but a solution with satisfactory consistency between -1 and +2 GeV^2 is obtained. The scale of energy is established by giving the ρ resonance the physical mass; the self-consistent ρ width is then about 400 MeV. Various dynamical approximations are investigated, and it is shown explicitly that the pion mass is not a significant parameter of the dynamics. Finally, a bootstrap calculation of both the ρ and Pomeranchuk trajectories is presented. Except for the Pomeranchuk residue, the results show satisfactory self-consistency throughout the range -1 to +2 GeV^2. The self-consistent Pomeranchuk trajectory has an intercept $\alpha_P(0) \approx 1$ and a slope $\alpha_P'(0) \approx 0.5$ GeV^{-2}.

singular, double integrals. In spite of this forbidding numerical prospect, the technique has received some attention.[9,10] It has conceptual, if not mathematical, simplicity, and it turns out that the real and imaginary parts of the leading Regge trajectories and their residues are easily computed above threshold. Some more technical problems of the N/D method, such as those associated with repulsive potentials like that due to Pomeranchuk exchange,[11] also appear to be circumvented. These difficulties are associated with the fact that the input to the N/D equations should in any case be unitarized by means of the Mandelstam iteration. This procedure has also been shown to be necessary in nonrelativistic potential scattering.[12]

It appears, then, that the Mandelstam iteration, as a basis for bootstrap calculations, has languished rather because of numerical difficulties than on account of any dynamical inadequacies. Considerable progress in the solution of these numerical problems was made by Bali,[10] who showed that results of adequate precision were obtained from a computer program that applied the Mandelstam iteration to nonrelativistic potential scattering. Bali also found that the method, with a particular cutoff prescription,[13] gave interesting results in relativistic calculations.

In this paper we report further progress in the numerical implementation of the Mandelstam iteration, made possible by the development of a new computer program that operates between five and ten times faster than those used in earlier calculations. This speed permits the laborious parameter searches inherent in bootstrap

calculations to be carried out without excessive use of computer time, and so it has become possible to apply this technique to the controversial $\pi\pi$ bootstrap problem.

A variety of bootstrap techniques have been applied to the problem of calculating the $\pi\pi$ scattering amplitude, generally with limited success. If only the $I = 1$ $\pi\pi$ channel is included, then a p-wave resonance can be bootstrapped, but its width is typically two or three times larger than that of the observed ρ resonance. This difficulty has persisted even in the most sophisticated single-channel calculations.[3] At the same time, studies of more massive channels, such as $\pi\omega$, KK^*, and $N\bar{N}$, have suggested that these channels do make large contributions in the formation of the ρ,[14] and that this particle should be regarded as predominantly an $N\bar{N}$ bound state.[15] However, recent calculations by Collins and Johnson[4,5] have disrupted this interpretation, since they appear to show that the proper inclusion of the $I = 0$ $\pi\pi$ channel suffices to reduce the ρ width to the observed value. Their prescription for the $I = 0$ scattering involves the exchange of the Pomeranchuk trajectory, which is treated as an ordinary Regge trajectory with an intercept $\alpha_p(0) \approx 1$.

Our approach to this problem has been, like that of Collins and Johnson, within the framework of the strip approximation. In Sec. II we set out the notation and assumptions of this approximation, which we use in Sec. III in a bootstrap calculation of the ρ trajectory. The results are similar to those of earlier calculations, although our technique allows us to impose strict requirements of self-consistency

above threshold, and in particular to arrive at a self-consistent value of the ρ width. The effects of various approximations are relatively easy to interpret in this simple one-trajectory calculation, and we study these effects in some detail. In Sec. IV we include the $I = 0$ $\pi\pi$ channel in a bootstrap calculation of the ρ and Pomeranchuk trajectories. We observe no tendency for the ρ width to be reduced by the inclusion of Pomeranchuk exchange. In Sec. V we summarize the results and discuss the disagreement between our observations and those of Collins and Johnson.

II. THE STRIP APPROXIMATION

We assume that the reader is familiar with the phenomenological arguments in favor of the strip approximation;[6] in this section we simply set down the equations that define the model, with only the briefest comments on their plausibility.

The Bose-symmetrized s-channel $\pi\pi$ scattering amplitude with isospin I, $A_s^I(s,t,u)$, may be written in the form

$$A_s^I(s,t,u) = A^I(s,t) + (-1)^I A^I(s,u), \tag{2.1}$$

where $A^I(s,t)$ is an amplitude of definite signature, having only right-hand singularities in the t plane. The normalization is such that the s-channel differential cross section is

$$\frac{d\sigma^I}{dt} = \frac{\pi}{sq_s^2} |A_s^I(s,t,u)|^2, \tag{2.2}$$

where $q_s = \frac{1}{2}(s - 4m_\pi^2)^{\frac{1}{2}}$ is the s-channel c.m. momentum.

The first assumption of the strip approximation is that an amplitude of definite signature has double spectral functions that are nonvanishing only in the strip regions A, B, C, and D of Fig. 1. Furthermore, it is assumed that the contribution of the shaded region A is given by the following s-channel elastic unitarity equation:

$$\rho_{out}^I(s,t) = \frac{g(s)}{\pi q_s s^{\frac{1}{2}}} \iint_{4m_\pi^2}^{K=0} dt_1 dt_2 \frac{D_t^{I*}(t_1,s)\, D_t^I(t_2,s)}{K^{\frac{1}{2}}(s;\, t,t_1,t_2)}, \tag{2.3}$$

where

$$K(s;\ t,t_1,t_2) = t^2 + t_1^{\,2} + t_2^{\,2} - 2(tt_1 + tt_2 + t_1t_2) - tt_1t_2/q_s^{\,2}, \tag{2.4}$$

and the t discontinuity of the amplitude, $D_t^{\,I}(t,s)$, is given by

$$D_t^{\,I}(t,s) = V_t^{\,I}(t,s) + \frac{1}{\pi}\int ds'\ \frac{\rho_{out}^{I}(s',t)}{s' - s} + \frac{\beta_{II}}{\pi}\int du'\ \frac{\rho_{out}^{I}(u',t)}{u' - u}, \tag{2.5}$$

where

$$V_t^{\,I}(t,s) = \sum_{I'}\ \beta_{II'}\left\{\frac{1}{\pi}\int ds'\ \frac{\rho_{in}^{I'}(t,s')}{s' - s} + \frac{(-1)^{I'}}{\pi}\int du'\ \frac{\rho_{in}^{I'}(t,u')}{u' - u}\right\}$$

$$+ \sum_{I'\neq I}\beta_{II'}\ \frac{(-1)^{I+I'}}{\pi}\int du'\ \frac{\rho_{in}^{I'}(u',t)}{u' - u}. \tag{2.6}$$

Here $\beta_{II'}$ is an isospin crossing matrix element, and $g(s)$ is a cutoff function[13] which forces the function $\rho_{out}^{I}(s,t)$ to vanish above the upper boundary $s = s_c$ of the strip A. This is not otherwise ensured by the equations, so the cutoff is assumed to represent some influence of other channels that causes the interior parts of the double spectral functions to be negligible. The interpretation of Eqs. (2.3) - (2.6) is as follows: one starts with input double spectral functions $\rho_{in}^{\,I}(s,t)$, for $I = 0$, 1, and 2, which specify a potential according to Eq. (2.6). This potential may be used in Eqs. (2.3) and (2.5) to generate the output functions $\rho_{out}^{I}(s,t)$, by means of the Mandelstam iteration procedure. In principle, one has only to find a set of

functions $\rho^I(s,t)$ such that

$$\rho_{in}{}^I(s,t) = \rho_{out}^I(s,t) = \rho^I(s,t), \tag{2.7}$$

for all s, t, and I, in order to have arrived at a complete solution of $\pi\pi$ scattering within the limitations of the strip approximation. The amplitude generated is not simply elastically unitary, since for example the strip B makes a contribution that represents a certain class of multipion unitarity contributions, namely those that have a t-channel elastic intermediate state. In this respect the $\pi\pi$ strip model bears a strong resemblance to the type of multiperipheral model proposed by Amati, Bertocchi, Fubini, Stanghellini, and Tonin.[16]

The goal of satisfying Eq. (2.7) at all s, t, and I is at present too ambitious, and in practice one attempts only to find functions containing the same leading s-channel Regge poles for some limited region of s:

$$\rho_{in}{}^I(s,t) \underset{t\to\infty}{\sim} \Delta_s\left\{\beta_{in}{}^I(s)\, t^{\alpha_{in}{}^I(s)}\right\}$$

and

$$\rho_{out}^I(s,t) \underset{t\to\infty}{\sim} \Delta_s\left\{\beta_{out}^I(s)\, t^{\alpha_{out}^I(s)}\right\}, \tag{2.8}$$

where

$$\left.\begin{aligned} &\alpha_{in}{}^I(s) \approx \alpha_{out}^I(s) \\ \text{and} \\ &\beta_{in}{}^I(s) \approx \beta_{out}^I(s) \end{aligned}\right\} \quad \text{over some limited range of } s. \tag{2.9}$$

Here Δ_s represents the discontinuity across the cuts associated with the s-channel threshold branch points. If these self-consistent trajectories resemble the observed ones, the amplitude will have the correct principal low-energy resonances and the correct behavior near the forward direction at higher energies, which would account for most of the features of the experimental data. However, we can hope to find such a solution only if the dynamics of $\pi\pi$ scattering are primarily determined in $\pi\pi$ channels, because the cutoff prescription is too crude to represent in detail any important contributions from other channels.

III. RHO BOOTSTRAP CALCULATION

For our first $\pi\pi$ bootstrap calculation we perform the standard single-channel calculation of the $I = 1$ amplitude. The input potential will involve the exchange of the ρ Regge trajectory, which is well known to provide the dominant forces in this system. However, ρ exchange also gives rise to strong forces in the $I = 0$ direct channel, so for real self-consistency one should include some $I = 0$ input, and in Sec. IV we shall do this.

We assume for the input double spectral function $\rho_{in}^{1}(s,t)$ a simple form that has a leading Regge trajectory $\alpha(s)$ with residue $\beta(s)$:

$$\rho_{in}^{1}(s,t) = \Delta_s \left\{ \beta(s)[(t + 2q_s^2)/s_0]^{\alpha(s)} \right\} \theta_1(t_c,\Delta,t), \qquad (3.1)$$

where s_0 is the conventional Regge scale factor of 1 GeV^2, and $\theta_1(t_c,\Delta,t)$ is the following continuous "effective threshold function":

$$\left.\begin{aligned} \theta_1(t_c,\Delta,t) &= 0 && t \leqslant t_c - \Delta \\ &= \tfrac{1}{2}[1 + (t - t_c)/\Delta] && t_c - \Delta < t < t_c + \Delta \\ &= 1 && t \geqslant t_c + \Delta. \end{aligned}\right\} \qquad (3.2)$$

The effect of the cutoff function θ_1 is to approximate the curved boundary of the physical double spectral function by a straight boundary near $t = t_c$, as shown in Fig. 1. We therefore regard t_c as a free parameter, representing the effective inelastic threshold of the potential, which may be varied to improve the self-consistency of a bootstrap solution. The function of the small parameter Δ is to remove a logarithmic singularity that would appear in the potential at

$s = t_c$ if the double spectral function were discontinuous. One finds, on substituting the form (3.1) in Eq. (2.6), that the potential is given by

$$V_t^{\,l}(t,s) = \Delta_t\left\{\frac{\beta(t)}{2\pi}\left[\frac{\tau_c(t)}{s_0}\right]^{\alpha(t)} R_{\alpha(t)}^{-}\left[\frac{s + 2q_t^{\,2}}{\tau_c(t)};\ \frac{2\Delta}{\tau_c(t)}\right]\right\}, \qquad (3.3)$$

where $\tau_c(t) = t_c - \Delta + 2q_t^{\,2}$; the function $R_\alpha^-(x;\ \epsilon)$ is defined by the relation

$$R_\alpha^{\pm}(x;\ \epsilon) = \frac{1}{\epsilon}\left\{R_{\alpha+1}^{\pm}(x) - R_\alpha^{\pm}(x) - (1+\epsilon)^{\alpha+1}\left[R_{\alpha+1}^{\pm}\left(\frac{x}{1+\epsilon}\right) - R_\alpha^{\pm}\left(\frac{x}{1+\epsilon}\right)\right]\right\}, \qquad (3.4)$$

where

$$R_\alpha^{\pm}(x) = \int_1^\infty dy\ y^\alpha\left(\frac{1}{y - x} \pm \frac{1}{y + x}\right). \qquad (3.5)$$

This integral may be expressed in terms of the hypergeometric function

$$R_\alpha^{+}(x) = -\frac{2}{\alpha} F\left(1,\ \frac{\alpha}{2};\ 1 - \frac{\alpha}{2};\ x^2\right) \qquad (3.6)$$

and

$$R_\alpha^{-}(x) = xR_{\alpha-1}^{+}(x), \qquad (3.7)$$

which permits the definition of the potential through analytic continuation for all s and t. In the limit $\Delta \to 0$, we have $\epsilon \to 0$ and $R_\alpha^{\pm}(x;\ \epsilon) \to R_\alpha^{\pm}(x)$; the potential is then logarithmically singular at $s = t_c$. A finite value of Δ removes this singularity, and the potential is then continuous throughout the neighborhood of $s = t_c$.

We parametrize the leading trajectory $\alpha(s)$ and its residue $\beta(s)$ in the following way:

$$\alpha(s) = a_\rho + bs + c(4m_\pi^2 - s)^p, \tag{3.8}$$

$$\beta(s) = g_\rho \; c_\rho^{\alpha(s)} \; \theta_2(s_c,\Delta,s)/\Gamma[\alpha(s)], \tag{3.9}$$

where $\theta_2(s_c,\Delta,s)$ is a cutoff function with a continuous derivative,

$$\left.\begin{aligned} \theta_2(s_c,\Delta,s) &= 1 && s \leqslant s_c - \Delta, \\ &= \tfrac{1}{4}\{2 + (s - s_c)[(s - s_c)^2 - 3\Delta^2]/\Delta^3\} \\ & && s_c - \Delta < s < s_c + \Delta, \\ &= 0 && s \geqslant s_c + \Delta. \end{aligned}\right\} \tag{3.10}$$

We use this cutoff function, rather than one similar to that in Eq. (3.2), because the numerical details of the Mandelstam iteration make it desirable that the potential should be fairly smooth in t. By choosing

$$g(s) = \theta_2(s_c,\Delta,s) \tag{3.11}$$

in Eq. (2.3), we ensure that the strip width is the same for the input and output double spectral functions. Apart from this cutoff factor, the form of the residue in Eq. (3.9) is just that given by the asymptotic form of the Veneziano formula for $\pi\pi$ scattering.[17] We take c_ρ to be a free parameter, although one might suppose that the Veneziano formula suggests the value $c_\rho = \alpha' s_0$, where α' is the mean trajectory slope. This would not be correct, because we ought to use

only the s-channel elastic contribution, rather than the complete Veneziano term, for the input potential. The value of c_ρ is therefore expected to be less than $\alpha' s_0$, corresponding to an elasticity that decreases with increasing s.

There are eight parameters to be varied in the search for a bootstrap solution: a_ρ, b, c, p, g_ρ, c_ρ, s_c, and t_c. We did not vary the cutoff width parameter Δ, since the dynamics are quite insensitive to its value, which we fixed at 0.5 GeV^2. For given values of the parameters, the Mandelstam iteration is carried out and the t discontinuity $D_t{}^I(t,s)$ is computed at successively higher values of t. Eventually the Regge asymptotic behavior becomes apparent:

$$D_t{}^I(t,s) \underset{t\to\infty}{\sim} \beta_{out}(s)[(t + 2q_s{}^2)/s_0]^{\alpha_{out}(s)} \tag{3.12}$$

[c.f. Eq. (3.1)], and the leading output trajectory $\alpha_{out}(s)$ and its residue $\beta_{out}(s)$ may be found by making least-squares linear fits to $\ell n\, D_t{}^I$ as a function of $\ell n[(t + 2q_s{}^2)/s_0]$. We find that local duality[18] holds in this situation, in the sense that these linear fits, extrapolated downward from very large t, also describe the average behavior of $\ell n\, D_t{}^I$ in the intermediate energy range (2 GeV$^2 \lesssim t \lesssim 20$ GeV^2). Conversely, a least-squares linear fit over an appropriate intermediate energy region, where $\ell n\, D_t{}^I$ may still exhibit pronounced oscillations, gives a good representation of the asymptotic behavior. It is usually possible, therefore, to determine the output Regge pole parameters in this intermediate t region, corresponding to 15-25 Mandelstam iterations, and to avoid making the

very large number of iterations, typically 50-70, necessary to reach the truly asymptotic t region.[10] An example of our procedure is illustrated in Fig. 2.

We chose to impose self-consistency on the ρ trajectory and residue in the region of s from -1 GeV^2 to +2 GeV^2, since one could not reasonably expect the strip approximation to be valid outside this range. In this region, a value of χ^2 is computed for the consistency of the input and output values of $Re(\alpha)$, $Im(\alpha)$, $Re(\beta)$, and $Im(\beta)$. The χ^2 contributions of the trajectory and the residue are weighted according to their expected relative numerical precision; it turns out that the residue is a good deal less accurately determined than the trajectory, so it receives less weight. A minimization program directs a parameter search that leads to the solution with the minimum value of χ^2.

The requirement that the real and imaginary parts of the trajectory and residue should be self-consistent above threshold is a very strict one that has not been imposed in any other bootstrap calculation. In the ρ bootstrap of Collins and Johnson,[3] for example, the inconsistency above threshold must be very great, since the widths of the input and output ρ resonances differ by a factor of at least 2. It is therefore not clear from earlier calculations that a ρ resonance of any self-consistent width can be generated.

We do in fact find a solution with fairly good self-consistency throughout the region of interest, which is shown in Fig. 3. In view of numerical errors of about 20% in the calculation of the residue function, the consistency is good below 1 GeV^2, although above this

value there is a significant tendency for the output value of $\mathrm{Re}\ \beta$ to decrease less rapidly than the input. There is a corresponding tendency for the output value of $\mathrm{Im}\ \alpha$ to rise rather too rapidly.

We do not find any solution that differs very much from that in Fig. 3; for example, the intercept of the self-consistent trajectory appears to be limited to the range $0.60 \lesssim \alpha(0) \lesssim 0.75$. This represents a considerable improvement in uniqueness over earlier ρ bootstrap calculations, presumably because of the requirement of consistency above threshold.

The isovector, p-wave cross section, corresponding to the solution in Fig. 3, is shown in Fig. 4. The consistency of input and output is good, but the ρ is wider, by a factor of about 3, than the experimentally observed resonance. As we discussed in Sec. I, the large width of the output ρ resonance has always been a problem in single-channel $\pi\pi$ bootstrap calculations, and by increasing the input width to achieve consistency we have not rectified this.

Our technique of calculation has some disadvantages if one needs to evaluate amplitudes and cross sections, because we can at present identify only the leading term in the asymptotic behavior of $D_t^I(t,s)$, that is, the leading output Regge pole. In calculating the amplitude,

$$A^I(s,t) = \frac{1}{\pi} \int_{4m_\pi^2}^{\infty} dt' \, \frac{D_t^I(t',s)}{t' - t} , \tag{3.13}$$

it is necessary to know the locations and residues of all poles in the right half of the angular momentum plane. However, insofar as the

amplitude calculated according to Eq. (3.13), taking into account only the leading Regge pole, lies on the unitary circle, we may say that we see no evidence of important secondary pole contributions for $s < 2$ GeV^2.

Figure 5 shows how some representative output quantities depend on the cutoff and threshold parameters s_c and t_c, when the other input parameters are held constant. Since t_c affects only the nonresonant contribution to the potential, which is dominated by the resonant ρ contribution, there is little sensitivity to the value of this parameter, and in fact we did not vary it in the search for a bootstrap solution, but held it constant at the value 2.73 GeV^2 ($= 150\ m_\pi^2$).

The sensitivity to the cutoff parameter s_c, on the other hand, is pronounced. This is reasonable, because the cutoff represents two important effects, which are presumably associated in the real world with inelastic channels not present in our model. The first of these is the elimination, through the function $g(s)$ in Eq. (2.3), of Regge cut contributions. This mechanism is discussed in detail in Ref. 13. The second effect is the decoupling, in Eq. (3.9), of the high-spin part of the input trajectory, which would otherwise play an unreasonably large role in the dynamics, even in the presence of the rapidly decreasing elasticity factor c_ρ^α. One may of course achieve the same effect by arranging for the input trajectory to turn over at some small value of α, but we have not chosen this scheme, because it would require much more elaborate parametrizations of both the trajectory and residue functions. However, the output trajectory does in fact turn

over in the upper half of the strip, so the output residue is not required to fall rapidly in order to decouple high output spins. This is probably the source of the disagreement of the input and output residues at high s, which may be seen in Fig. 3.

The magnitude of the pion mass is of crucial importance in the Mandelstam iteration procedure, since the number of iterations required to continue the double spectral function to a given value of t is inversely proportional to this quantity. One might suppose, therefore, that the scale of energy in our calculations is set by the pion mass, which would then be a dynamical quantity of great significance. Figure 6 shows that this is not the case. For given input parameter values, the output is largely insensitive to the pion mass, provided this is less than about 0.2 GeV. Of course the Mandelstam iteration becomes numerically unreliable if the pion mass is too small, owing to the large number of iterations required to reach the region of large t. The apparent variation in the output below $m_\pi = 0.08$ GeV can be ascribed to numerical difficulties of this type. On the other hand, there does appear to be an onset of significant variation around $m_\pi = 0.18$ GeV, corresponding to the $\pi\pi$ threshold lying one full width below the ρ pole. Presumably a more realistic calculation, with a narrower ρ resonance, would show no variation up to even larger values of the pion mass. These considerations suggest that, although the nonzero pion mass is an important kinematic feature that makes the Mandelstam iteration possible, its neglect does not lead to any significant distortion of the dynamics of $\pi\pi$ scattering.

A direct result of the insensitivity to the pion mass is the existence of a continuum of bootstrap solutions, related to the one in Fig. 3 by a change in the energy scale of the input parameters. We have fixed this scale by setting the input ρ mass at approximately the physical value. When the resonance width is large, this does not correspond to the condition $\mathrm{Re}\,\alpha(m_\rho^2) = 1$, but to a more complicated condition given, for example, by Newton.[19]

The dynamical effects of the strip labelled D in Fig. 1 are expected to be small in the region $s \gtrsim -1\ \mathrm{GeV}^2$, because the potential contribution of this strip contains no resonances at low t and behaves like $t^{\alpha(-t)}$ at high t. In a single-channel calculation, the strip D contribution enters only as the last term in Eq. (2.5), and in Fig. 7 we show that the effect of neglecting this term is indeed small. In a two-channel calculation, with both $I = 0$ and $I = 1$, strip D contributions also occur in Eq. (2.6), where they have to be computed in terms of the input double spectral functions $\rho_{in}^{I}(s,t)$. If these contributions are to be included, our input trajectory parametrization must be modified, because the form (3.8) gives $\alpha(-t) \to +\infty$ as $t \to \infty$. However, we take the evidence of Fig. 7 to indicate that all strip D contributions are negligible, and in the two-channel calculation of Sec. IV we shall omit them altogether.

IV. INCLUSION OF THE POMERANCHUK TRAJECTORY

A simple inspection of the $\pi\pi$ isospin crossing matrix reveals that ρ exchange produces a strong attractive force in the $I = 0$ direct channel, and this force gives rise to a high-lying output trajectory with the quantum numbers of the vacuum. We display in Fig. 8 the position and residue of this Pomeranchuk trajectory for the pure $I = 1$ input of the ρ bootstrap calculation discussed in the previous section. The trajectory is roughly parallel to the output ρ trajectory, with very nearly the same imaginary part for $s < 2$ GeV^2, and with an intercept of about 1. The residue function has the same form as that for the ρ, but is about twice as large.

Since the potential is expected to be dominated by ρ exchange, the output Pomeranchuk trajectory should be similar to that shown in Fig. 8 even when Pomeranchuk exchange is included in the input. Accordingly, we have chosen the following parametrization of the input Pomeranchuk trajectory and its residue, corresponding to Eqs. (3.8) and (3.9) for the input ρ:

$$\alpha_P(s) = a_P + bs + c(4m_\pi^2 - s)^p, \tag{4.1}$$

$$\beta_P(s) = g_P \, c_P^{\alpha_P(s)} \, \theta_2(s_c,\Delta,s)/\Gamma[\alpha_P(s)], \tag{4.2}$$

where the parameters b, c, p, s_c, and Δ are the same as those for the input ρ trajectory. The $I = 0$ contribution to the potential then has a form similar to that given by Eq. (3.3), with the positive-signature function $R^+_{\alpha_P}$ in the place of R^-_α.

There are now 11 input parameters, namely a_ρ, a_P, b, c, p, g_ρ, g_P, c_ρ, c_P, s_c, and t_c, subject to the single constraint that the ρ resonance should have the physical mass. Figure 9 shows the most consistent solution that we have found using this parametrization. The agreement between input and output ρ and Pomeranchuk trajectories is good throughout the range $-1\ \text{GeV}^2 < s < 2\ \text{GeV}^2$, and the consistency of the ρ residue is rather better than in the single-channel calculation of Sec. III. However, even allowing for a 30% numerical uncertainty in the Pomeranchuk residue, the self-consistency of this quantity is unsatisfactory for $s \gtrsim 0.5\ \text{GeV}^2$.

The discrepancy between the input and output Pomeranchuk residues above $s \approx 0.5\ \text{GeV}^2$ reflects a difficulty of the strip approximation which we do not believe to be caused by our particular form of parametrization. For a wide variety of physically reasonable input potentials, the output Pomeranchuk residue falls rather slowly at large s, while the real and imaginary parts of the trajectory rise sufficiently rapidly that there is a significant f-meson contribution to the output cross section, even if the real part of the trajectory does not reach the value $\text{Re}(\alpha_P) = 2$. Correspondingly, if the input and output trajectories and residues are to agree up to $s \approx 2\ \text{GeV}^2$, there must be a large f-meson contribution to the input potential. As in potential scattering, such a high-mass exchange (short-range potential) generates output trajectories that are much too flat to bear any resemblance to those observed experimentally. The f meson must therefore be decoupled by an input residue that falls rapidly at large

s, and we have the residue discrepancy that appears in Fig. 9. Alternatively, the f contribution may be removed by making the input trajectory turn over at small s, but this leads to a comparable inconsistency with the output trajectory above $s \approx 0.5$ GeV^2. Clearly, this is another case of the problem of decoupling high-spin input contributions, as discussed in Sec. III. The problem is more serious here simply because the f resonance should in fact occur within our region of interest, $s < 2$ GeV^2.

The slope of the output ρ trajectory near $s = 0$ is similar to the observed value $\alpha'_\rho(0) \approx 0.9$ GeV^{-2}, but this is largely due to a threshold effect associated with the rapidly rising imaginary part of the trajectory. Above threshold the slope remains slightly greater than that obtained when Pomeranchuk exchange is ignored, but the effect of this on the width of the ρ resonance is overwhelmed by the increase in the imaginary part of the trajectory. The p-wave cross section, shown in Fig. 10, reveals that the ρ width is now about 600 MeV.

In Fig. 11 we exhibit the relevant behavior of the $I = 1$ output as the amount of input Pomeranchuk exchange is increased from zero. The trajectory intercept falls steadily, while the value of $\mathrm{Re}\,\alpha_\rho(0.5\ \mathrm{GeV}^2)$ is not substantially changed, so the real part of the output trajectory approaches a form with the physical slope and intercept. But the residue increases rapidly, not only for $s = 0$ (the representative value shown in Fig. 11) but also for $s > 0$, where a corresponding increase in $\mathrm{Im}\,\alpha$ produces the large width of the output resonance. In contrast to these observations, Collins and Johnson found in their

N/D calculations[4,5] that the inclusion of Pomeranchuk exchange led to a decrease in the ρ residue and to an associated reduction of the resonance width to the experimentally observed value.

Next we turn to a comparison of the self-consistent Pomeranchuk trajectory with the experimental data. The intercept $\alpha_P(0) \approx 1$ and the slope $\alpha_P' \approx 0.5$ GeV^{-2}, throughout the region -0.5 GeV$^2 < s \leqslant 0$, are in agreement with the values suggested by the recent Serpukhov pp scattering data.[20] The value of the residue at $s = 0$, however, corresponds [when we take $\alpha_P(0) = 1$] to an asymptotic $\pi\pi$ total cross section of 46 mb, whereas the estimate by factorization of the πp and pp data is 15-20 mb.

Chew and Snider[21] have conjectured, on the basis of their "schizophrenic pomeron" model, that a calculation of the type presented here should give rise to a degenerate leading $I = 0$ trajectory, which will be split in a more sophisticated scheme (involving small potential contributions not confined to the strip regions of Fig. 1) into two components corresponding to the physical P and P' trajectories. In order to split into P and P' components with the observed properties, the degenerate trajectory should have an intercept of about 0.7, the normal slope ($\approx$0.9 GeV^{-2}), and a large residue (about twice that of the P component). Although we find that the residue has roughly the expected size, the trajectory slope and intercept are more like those of an already-split P component. In view of our poor results on the ρ trajectory, which is not subject to such effects, this probably casts more doubt on the validity of the present form of the strip approximation than on the conjecture of Chew and Snider.

Our results on the intercept and residue of the Pomeranchuk trajectory are similar to those of Collins and Johnson, but they arrived at a higher, more normal, value of the slope, $\alpha_P' \approx 0.9$ GeV^2. They saw no sign of a secondary P' trajectory, as one would expect if their leading trajectory was degenerate.

As explained in Sec. III, our technique is not directly sensitive to secondary output trajectories. However, if one tries to use Eq. (3.13) to compute the isoscalar amplitude, subtracting out only the leading Regge pole on the right-hand side, one obtains an absurd result that appears to violate unitarity. This suggests the presence of a secondary pole with a positive intercept, and it is possible that further work along these lines will enable us to obtain quantitative information on secondary contributions of this type. In the meantime, we have no way of evaluating the isoscalar amplitude and, in particular, we are not able to compute an $I = 0$, $\ell = 0$ scattering length for comparison with the encouraging results of Collins and Johnson.[4]

As in the ρ bootstrap calculation of the previous section, there is in this case only a small range of solutions that are roughly as good as the one displayed in Fig. 9. We have not found any self-consistent trajectories with intercepts outside the ranges $0.55 \lesssim \alpha_\rho(0) \lesssim 0.70$, $0.90 \lesssim \alpha_P(0) \lesssim 1.05$; for solutions with intercepts within this range, we find $11 \lesssim \beta_P(0) \lesssim 17$.

We end this section with a brief discussion of the behavior of the ρ residue function near the wrong-signature point $\alpha_\rho = 0$. In Fig. 12 the trajectory and residue of Fig. 9 are extended into the

region $s < -1$ GeV^2, where no attempt was made to achieve self-consistency. The numerical errors are large in this region, because the asymptotic value of $D_t^1(t,s)$ there is very small compared with values in the strip region A. However, it is clear that the output trajectory passes through zero somewhere near $s = -1.7$ GeV^2, while the residue shows no sign of vanishing or even becoming small around this value of s. In other words, we detect no tendency for the dynamics to generate a zero of the output residue, and this of course precludes any possibility of self-consistency in this region, since we have used an input residue parametrization that does contain this zero. One might suppose that this difficulty causes a reduction of the slope of the self-consistent ρ trajectory, by forcing the point $\alpha_\rho = 0$ to lie outside the region ($s > -1$ GeV^2) in which consistency is demanded. But we find that ignoring the residue inconsistency, or requiring consistency only for $s > -0.5$ GeV^2, leads to little change in the trajectory slope, which is therefore not seriously constrained by this effect. Certainly our calculation would be more satisfactory if we could find a simple input ρ residue parametrization that does not vanish when $\alpha_\rho = 0$ but does lead to some self-consistent bootstrap solution. So far, however, we have not been able to do this, and, in any case, it appears unlikely that such a modification would remedy the basic problem of the large width of the ρ resonance.

V. CONCLUSIONS

In the preceding sections we hope to have shown that the Mandelstam iteration is a useful technique for performing detailed bootstrap calculations, and that it supplements the N/D method by providing valuable information on Regge trajectories above threshold. We have used the technique, in conjunction with the strip approximation, to carry out first a bootstrap calculation of the ρ trajectory alone, and then a combined bootstrap of the ρ and Pomeranchuk trajectories. We begin this section with a summary of the results of these calculations.

In the ρ bootstrap calculation there does exist a solution with satisfactory self-consistency in the region $-1\ \text{GeV}^2 < s < 2\ \text{GeV}^2$, but the trajectory slope is too small and the ρ resonance is about three times too wide. The strip width is an important parameter and has the value $3.64\ \text{GeV}^2$. If the strip width is increased, large contributions of the high-spin parts of the input trajectory are introduced. It does not seem possible to incorporate highly elastic high-spin resonances in the present formulation of the strip model, and problems associated with the existence of such resonances, like the g(1660), seem likely to occur in a large class of models.[22]

When Pomeranchuk exchange is included in the calculation, both the ρ and Pomeranchuk trajectories may be made reasonably self-consistent in the range $-1\ \text{GeV}^2 < s < 2\ \text{GeV}^2$, except for some inconsistency in the Pomeranchuk residue at positive s, which is associated with the high-spin resonance problem again, this time in connection with the f-meson contribution. The slope of the ρ trajectory is

slightly greater than in the calculation without Pomeranchuk exchange, but this is offset by a more rapid increase in the imaginary part above threshold, which leads to an even greater width for the ρ resonance.

The slope and intercept of the self-consistent Pomeranchuk trajectory are in agreement with experiment, but the residue is too large, and it appears likely that a valid strip approximation should in fact generate a leading $I = 0$ trajectory with just such a large residue, but with a normal slope and an intercept of about 0.7, which would be split by nonstrip effects into the observed P and P' trajectories. We have to conclude that the addition of the $I = 0$ $\pi\pi$ channel to our original single-channel calculation has not significantly increased our understanding of the details of $\pi\pi$ scattering.

The most natural conclusion from this rather disappointing result is that $\pi\pi$ scattering dynamics cannot in fact be understood in terms of the $\pi\pi$ channels alone. The large width that is obtained for the ρ suggests that this particle is in large measure a bound state of some channel of higher mass, such as $N\bar{N}$. Furthermore, the rather unsatisfactory way in which the cutoff prescription deals with the problem of high-spin resonances suggest that at least some of the inelastic effects, which the cutoff represents, must be handled explicitly through the inclusion of inelastic channels.

The bootstrap calculations of Collins and Johnson[3-5] are based on a formulation of the strip approximation that is very similar to ours, and, apart from some details due to the different parametrizations and regions of self-consistency, one would expect our results to be much the same as theirs. In the ρ bootstrap calculation this is indeed

the case.[23] However, as we have pointed out in Sec. IV, on including Pomeranchuk exchange we obtain substantially different results, for their solution displays many features of the experimental data, and in particular they find that the ρ resonance width is reduced to the physical value.

At present the reasons for this discrepancy remain obscure. Lyth[24] has argued that certain features of the results of Collins and Johnson suggest that the physical ρ should appear as a CDD pole in their $\pi\pi$ N/D equations. This would support our characterization of the ρ as primarily a bound state of some other channel. However, Bali, Chew, and Chu[13] have shown that the type of calculation presented here should be equivalent to an N/D calculation with no CDD parameters. For this reason, independent of the true nature of the ρ, one would expect the two calculations to give similar results.

ACKNOWLEDGMENTS

It is a great pleasure to acknowledge the innumerable helpful comments and criticisms of Geoffrey F. Chew. I am also grateful to Naren F. Bali and Cristian Sorensen for valuable conversations, and to Daniel P. Lamb for his elegant machine-language programming.

FOOTNOTES AND REFERENCES

* This work was supported in part by the U. S. Atomic Energy Commission.

1. G. F. Chew and S. C. Frautschi, Phys. Rev. Letters 7, 394 (1961).

2. Attempts to bootstrap Regge trajectories are discussed by P. D. B. Collins and E. J. Squires, Regge Poles in Particle Physics (Julius Springer-Verlag, Berlin, 1968); earlier calculations are reviewed by F. Zachariasen, in Recent Developments in Particle Physics, eidted by M. J. Moravcsik (Gordon and Breach, Science Publishers, Inc., New York, 1966), p. 86.

3. P. D. B. Collins and R. C. Johnson, Phys. Rev. 177, 2472 (1969).

4. P. D. B. Collins and R. C. Johnson, Phys. Rev. 182, 1755 (1969).

5. R. C. Johnson and P. D. B. Collins, Phys. Rev. 185, 2020 (1969).

6. G. F. Chew and S. C. Frautschi, Phys. Rev. 123, 1478 (1961).

7. G. F. Chew and S. Mandelstam, Phys. Rev. 119, 467 (1960).

8. S. Mandelstam, Phys. Rev. 112, 1344 (1958).

9. B. M. Bransden, P. G. Burke, J. W. Moffatt, R. G. Moorhouse, and D. Morgan, Nuovo Cimento 30, 207 (1963).

10. N. F. Bali, Phys. Rev. 150, 1358 (1966).

11. G. F. Chew and V. L. Teplitz, Phys. Rev. 137, B139 (1965).

12. P. D. B. Collins and R. C. Johnson, Phys. Rev. 169, 1222 (1968).

13. N. F. Bali, G. F. Chew, and S.-Y. Chu, Phys. Rev. 150, 1352 (1966).

14. J. S. Ball and M. Parkinson, Phys. Rev. 162, 1509 (1967).

15. S. Mandelstam, Phys. Rev. 166, 1539 (1968).

16. D. Amati, S. Fubini, A. Stanghellini, and M. Tonin, Nuovo Cimento 22, 569 (1961); L. Bertocchi, S. Fubini, and M. Tonin, Nuovo

Cimento 25, 626 (1962); D. Amati, A. Stanghellini, and S. Fubini, Nuovo Cimento 26, 896 (1962).

17. J. A. Shapiro, Phys. Rev. 179, 1345 (1969).

18. R. Dolen, D. Horn, and C. Schmid, Phys. Rev. 166, 1768 (1968).

19. R. G. Newton, The Complex J-Plane (W. A. Benjamin, Inc., New York, 1964), p. 9.

20. G. G. Beznogikh, A. Buyak, K. I. Iovchev, L. F. Kirillova, P. K. Markov, B. A. Morozov, V. A. Nikitin, P. V. Nomokonov, M. G. Shafranova, V. A. Sviridov, Truong Bien, V. I. Zayachki, N. K. Zhidkov, L. S. Zolin, S. B. Nurushev, and V. L. Solovianov, Phys. Letters 30B, 274 (1969).

21. G. F. Chew and D. R. Snider, Phys. Rev. D1, 3453 (1970).

22. P. D. B. Collins, R. C. Johnson, and E. J. Squires, Phys. Letters 26B, 223 (1968).

23. One should notice that the strip width, in the sense of the width of the regions outside which the double spectral functions are negligible, is determined in the Collins-Johnson calculations by the parameter they call t_α, which has a value of 2-3 GeV^2, in agreement with the value of our parameter s_c. The parameter s_1, which they refer to as the strip boundary, serves mainly as a point of transition from the low-energy to the asymptotic region.

24. D. H. Lyth, CERN TH-1143, March 1970.

FIGURE CAPTIONS

Fig. 1. The regions of the double spectral functions that are taken into account in the strip approximation to $\pi\pi$ scattering, and the cutoff and threshold parameters s_c and t_c.

Fig. 2. Examples of the fitting procedure used to compute the parameters of the leading output Regge trajectory. The dashed lines indicate the least-squares fits and the regions of t that were used, for the two cases $s = 0$ and $s = 2$ GeV^2. In this example the slope and intercept of the linear fit give the values of $\mathrm{Re}\,\alpha_\rho$ and $\ell n|\beta_\rho|$ at that value of s. The maximum value of t used in these fits ($t = 42$ GeV^2) corresponds to 22 Mandelstam iterations.

Fig. 3. The self-consistent ρ trajectory $\alpha(s)$ and its residue function $\beta(s)$. The input is shown by the dashed lines and the output by the full lines. Input parameter values were $a_\rho = 0.63$, $b = 1.22$ GeV^{-2}, $c = 0.92$ GeV^{-2p}, $p = 1.111$, $g_\rho = 63.4$, $c_\rho = 0.091$, $s_c = 3.64$ GeV^2, $t_c = 2.73$ GeV^2, $\Delta = 0.5$ GeV^2.

Fig. 4. Input (dashed line) and output (full line) isovector p-wave cross sections, corresponding to the solution shown in Fig. 3. The input ρ resonance has $m_\rho = 0.765$ GeV, $\Gamma_\rho = 0.410$ GeV, and the output has $m_\rho = 0.720$ GeV, $\Gamma_\rho = 0.415$ GeV.

Fig. 5. Dependence of the output values of the three representative quantities $\alpha(0)$, $\mathrm{Re}\,\alpha(0.5\ \mathrm{GeV}^2)$, and $\beta(0)$ on the parameters (a) s_c, (b) t_c. In each case the remaining input parameters

had the values given in the caption to Fig. 3, and the dashed lines indicate the corresponding input trajectory and residue values.

Fig. 6. Dependence of the output values of $\alpha(0)$, Re $\alpha(0.5\ \mathrm{GeV}^2)$, and $\beta(0)$ on the pion mass. The input values are shown by the dashed lines, and correspond to the input parameter values given in the caption to Fig. 3, apart from negligible changes due to the shift in the $\pi\pi$ threshold.

Fig. 7. Effects of neglecting the contribution due to strip D of Fig. 1. The input was as in Fig. 3; output with strip D contribution = ——, without strip D contribution = — - — -.

Fig. 8. Output Pomeranchuk trajectory and residue generated by the I = 1 input of Fig. 3.

Fig. 9. Self-consistent ρ and Pomeranchuk trajectories and their residue functions. The input is shown by the dashed lines and the output by the full lines. Input parameter values were $a_\rho = 0.59$, $a_P = 0.95$, $b = 1.45\ \mathrm{GeV}^{-2}$, $c = 1.15\ \mathrm{GeV}^{-2p}$, $p = 1.136$, $g_\rho = 33.2$, $g_P = 101.0$, $c_\rho = 0.22$, $c_P = 0.135$, $s_c = 2.8\ \mathrm{GeV}^2$, $t_c = 2.1\ \mathrm{GeV}^2$, $\Delta = 0.4\ \mathrm{GeV}^2$.

Fig. 10. Input (dashed line) and output (full line) isovector p-wave cross sections corresponding to the ρ trajectory and residue shown in Fig. 9. The large width and asymmetrical shape of the ρ resonance make its parameters difficult to determine. The input has $m_\rho \approx 0.76$ GeV, $\Gamma_\rho \approx 0.6$ GeV, while the output has $m_\rho \approx 0.71$ GeV, $\Gamma_\rho \approx 0.6$ GeV.

Fig. 11. Behavior of the output quantities $\alpha_\rho(0)$, Re $\alpha_\rho(0.5\ \mathrm{GeV}^2)$, and $\beta_\rho(0)$ when the amount of Pomeranchuk exchange is varied. All input parameters except g_P were held constant at the values given in the caption to Fig. 9.

Fig. 12. Input (dashed line) and output (full line) ρ trajectory and residue functions in the region of negative s. The numerical errors in this region are large, and no attempt was made to obtain self-consistency there, but the fact that the output residue remains large when the trajectory passes through zero is significant.

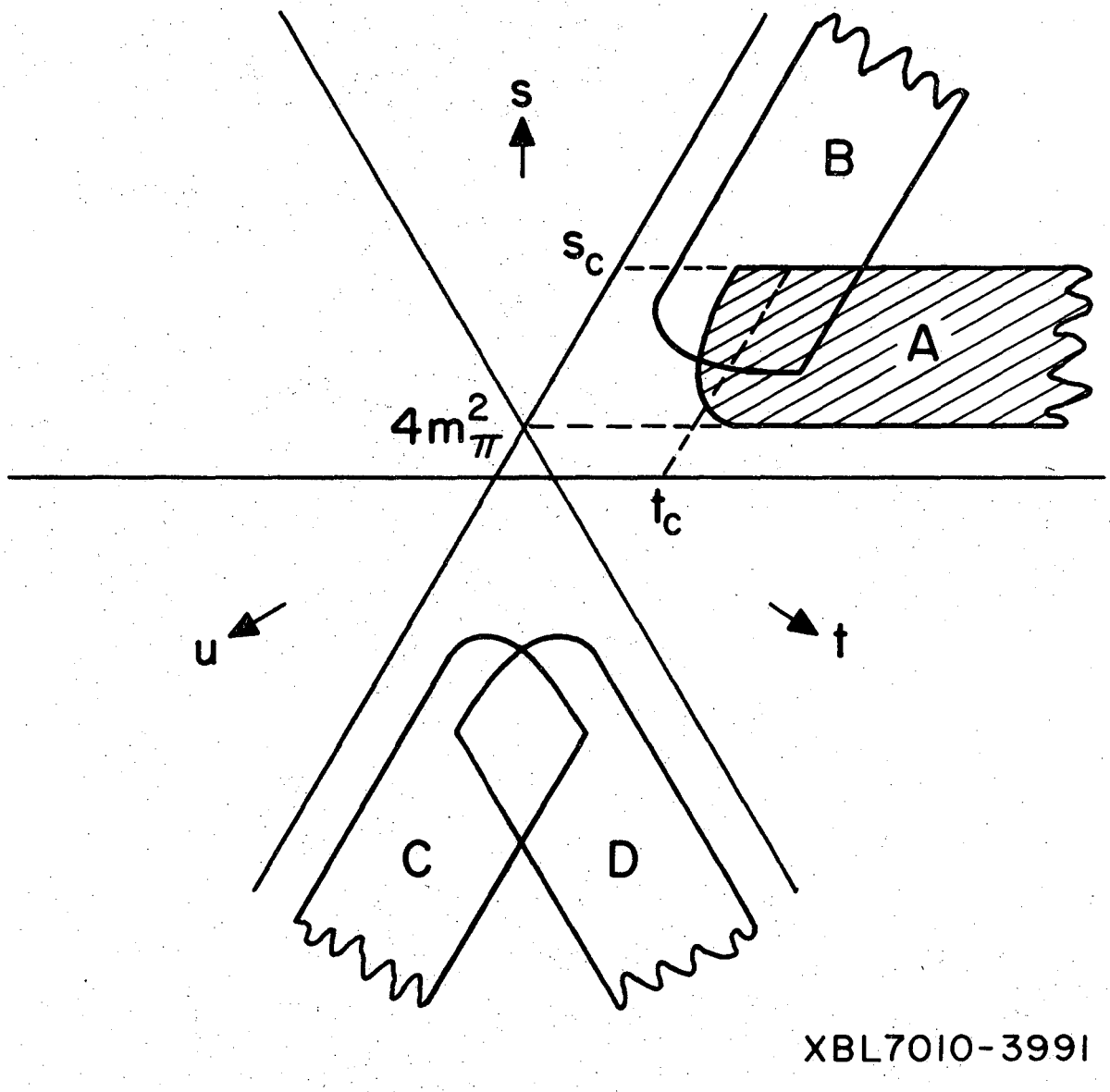

Fig. 1

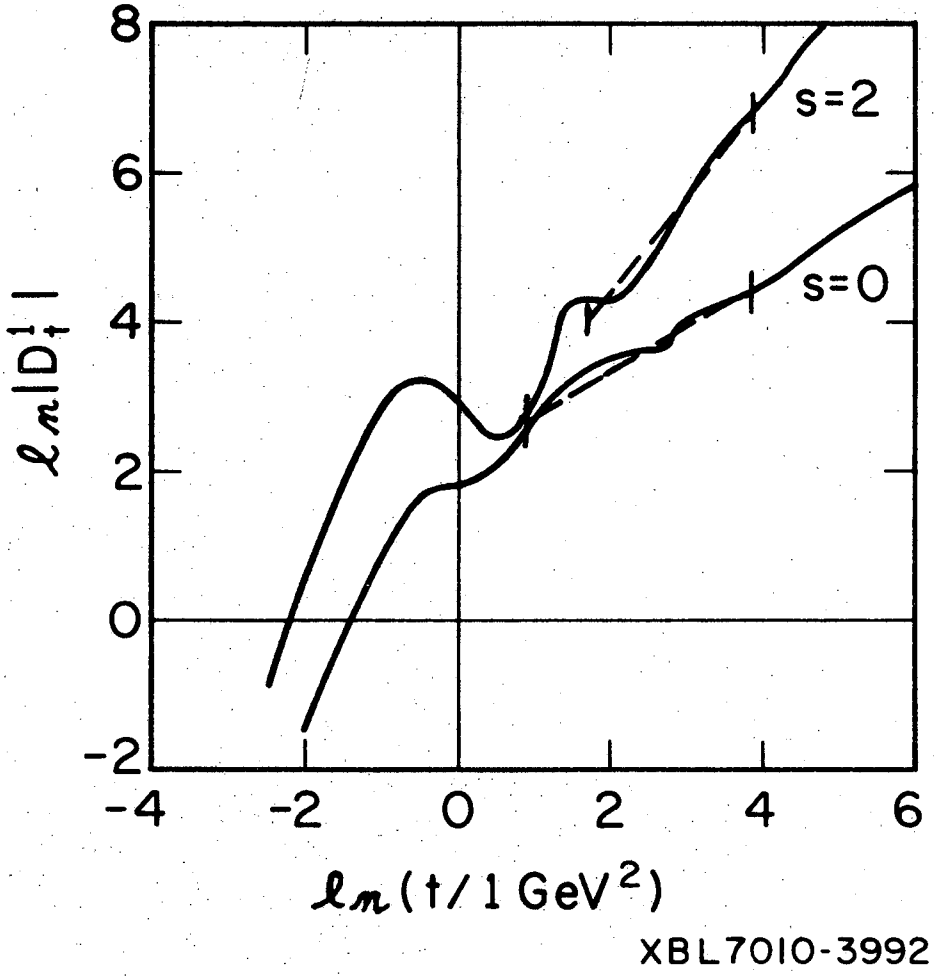

Fig. 2

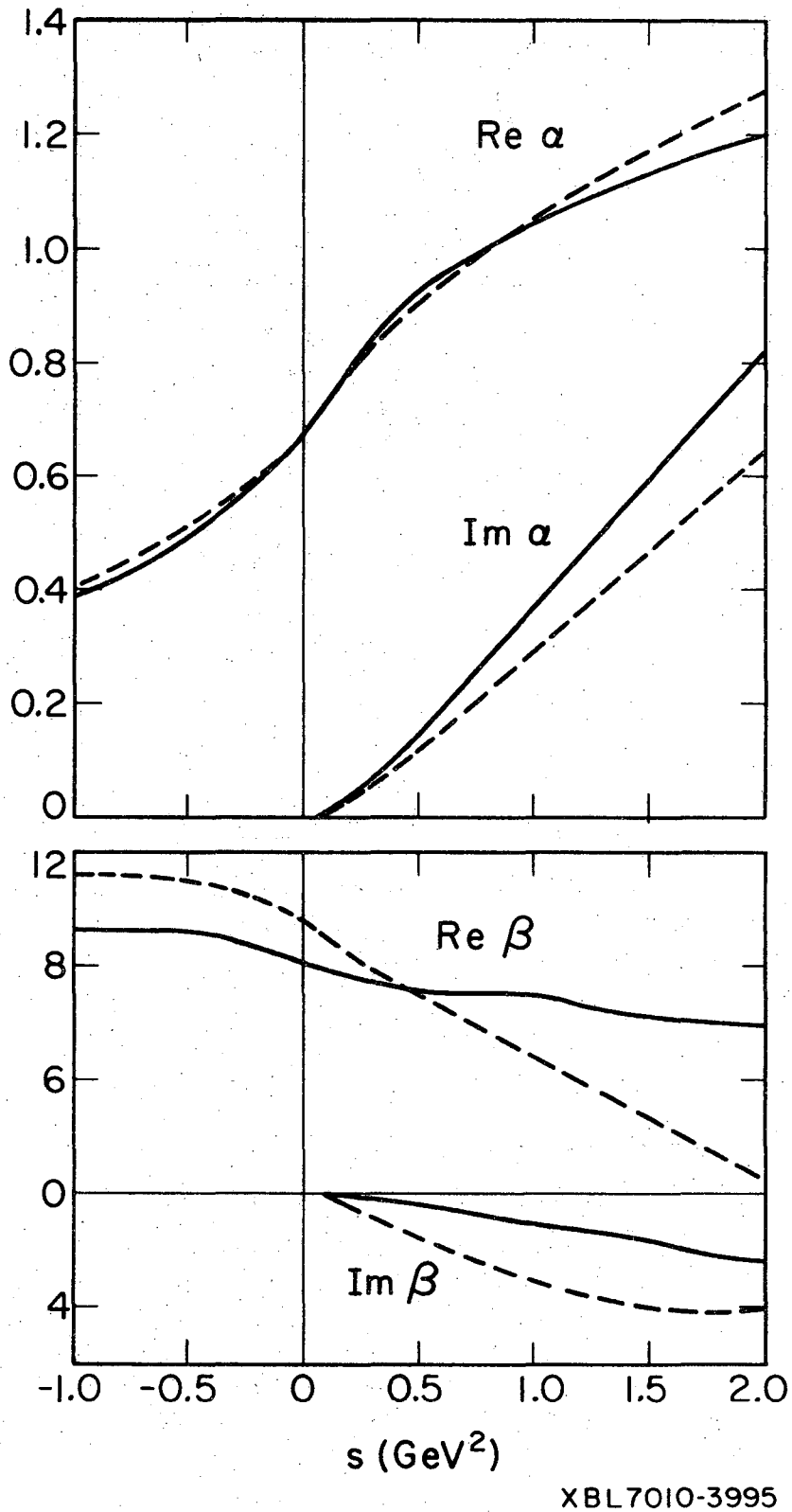
1.4
1.2
1.0
0.8
0.6
0.4
0.2
0
Re α
Im α
12
8
6
0
4
Re β
Im β
-1.0
-0.5
0
0.5
1.0
1.5
2.0
s (GeV²)
XBL7010-3995

Fig. 3

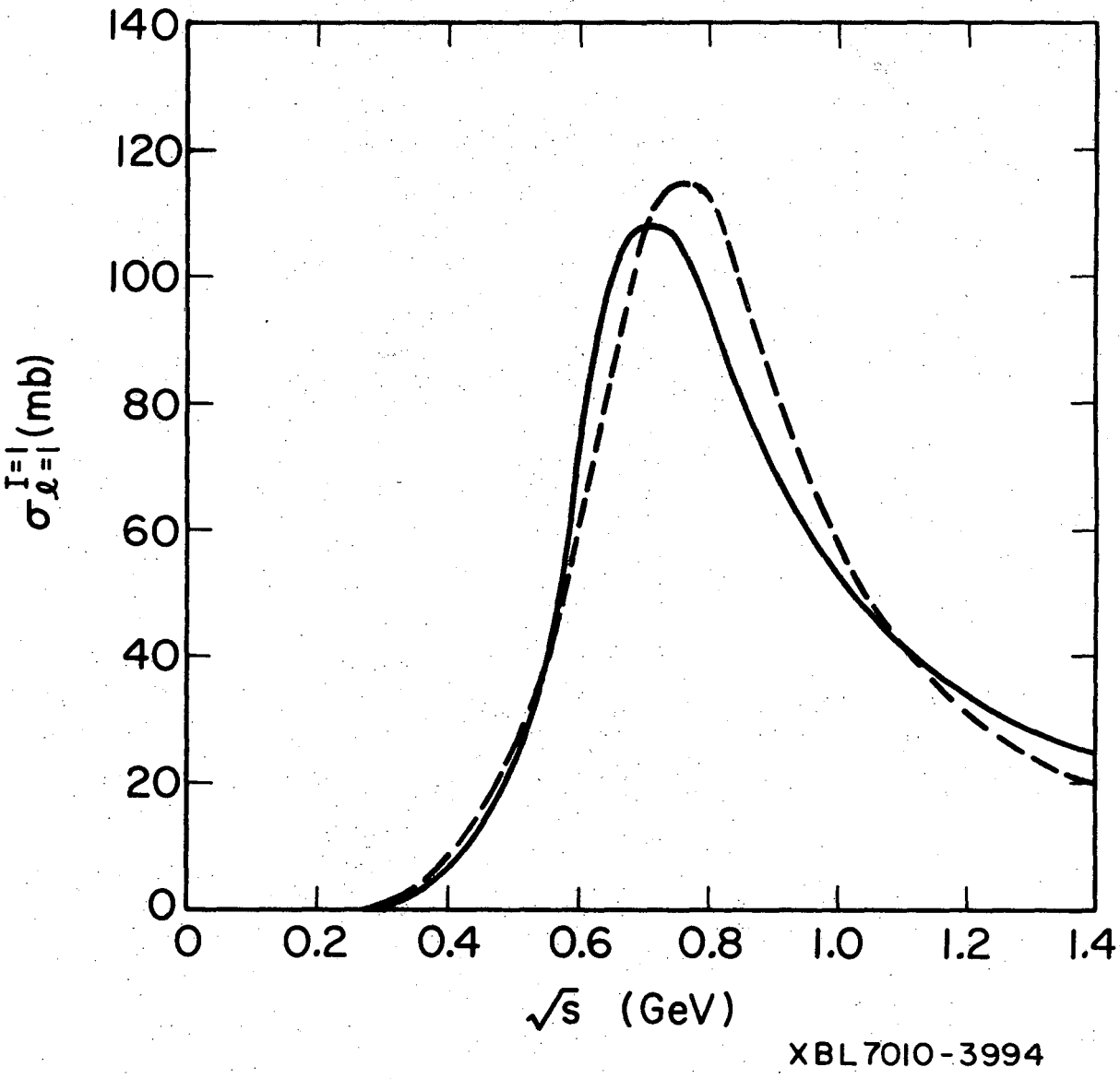
140
120
100
80
60
40
20
0
0
0.2
0.4
0.6
0.8
1.0
1.2
1.4
$\sigma_{\ell=1}^{I=1}$ (mb)
$\sqrt{s}$ (GeV)
XBL7010-3994

Fig. 4

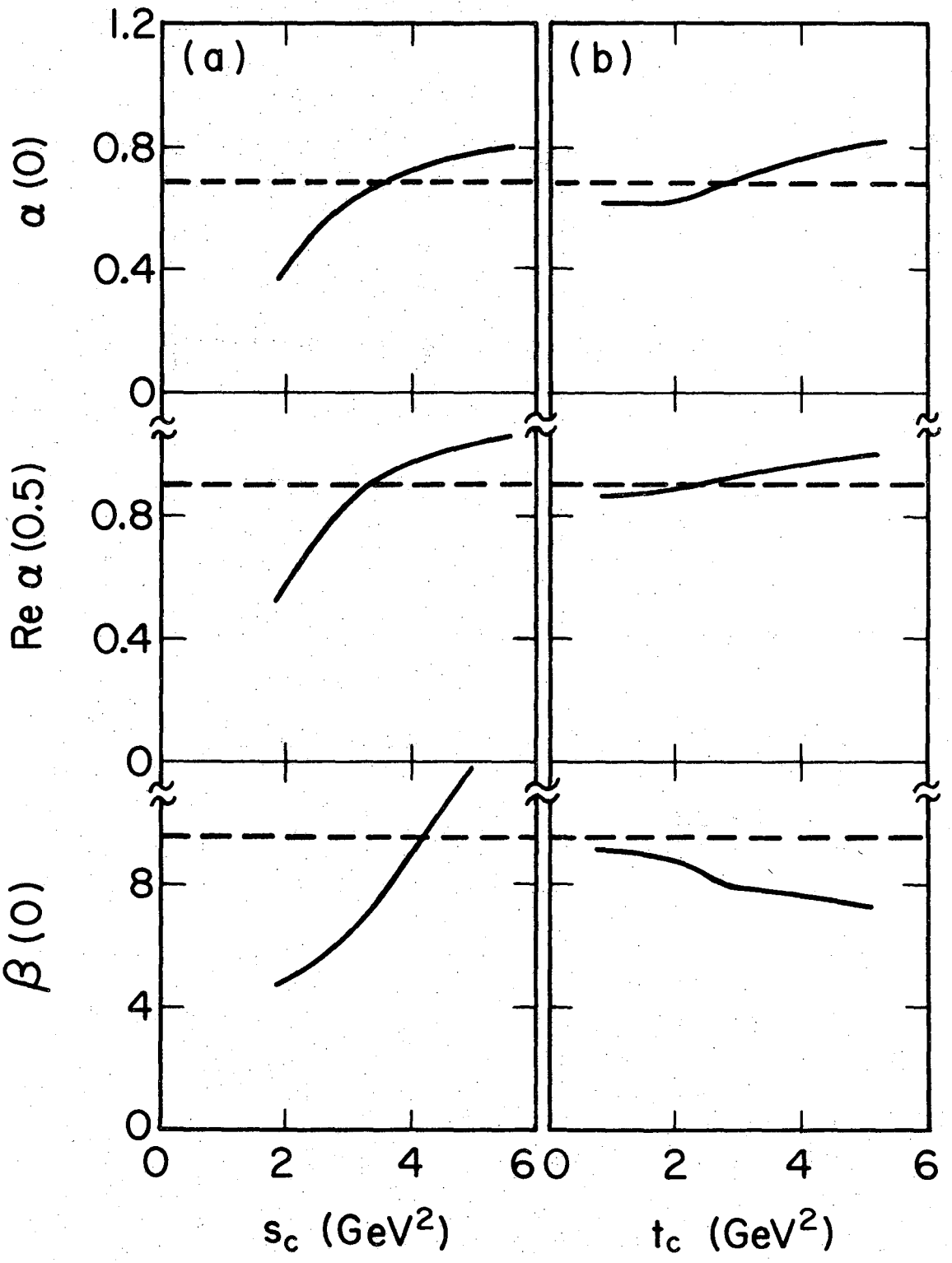

Fig. 5

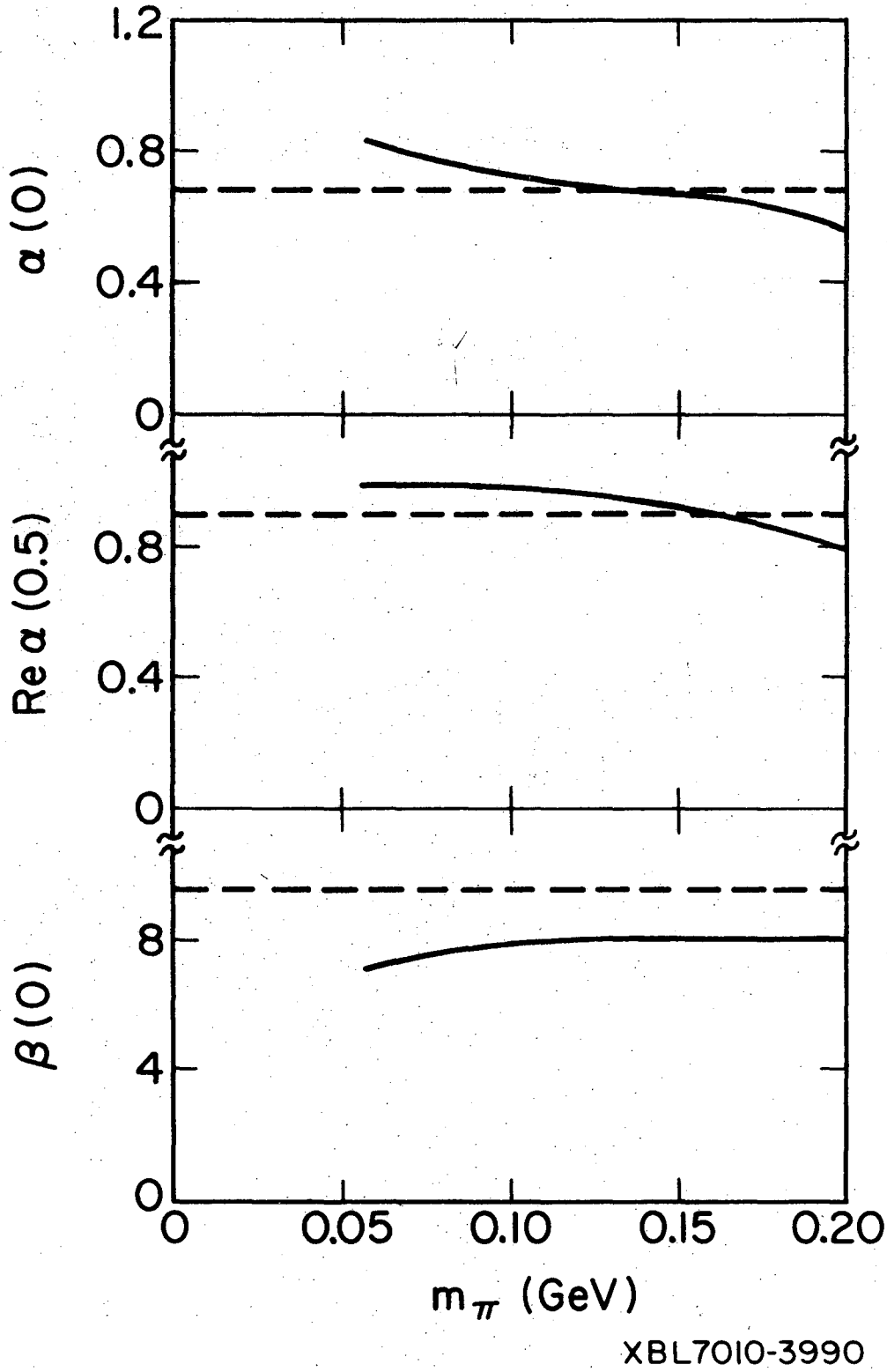
1.2
0.8
0.4
0
α(0)
0.8
0.4
0
Re α (0.5)
8
4
0
β(0)
0
0.05
0.10
0.15
0.20
m_π (GeV)
XBL7010-3990

Fig. 6

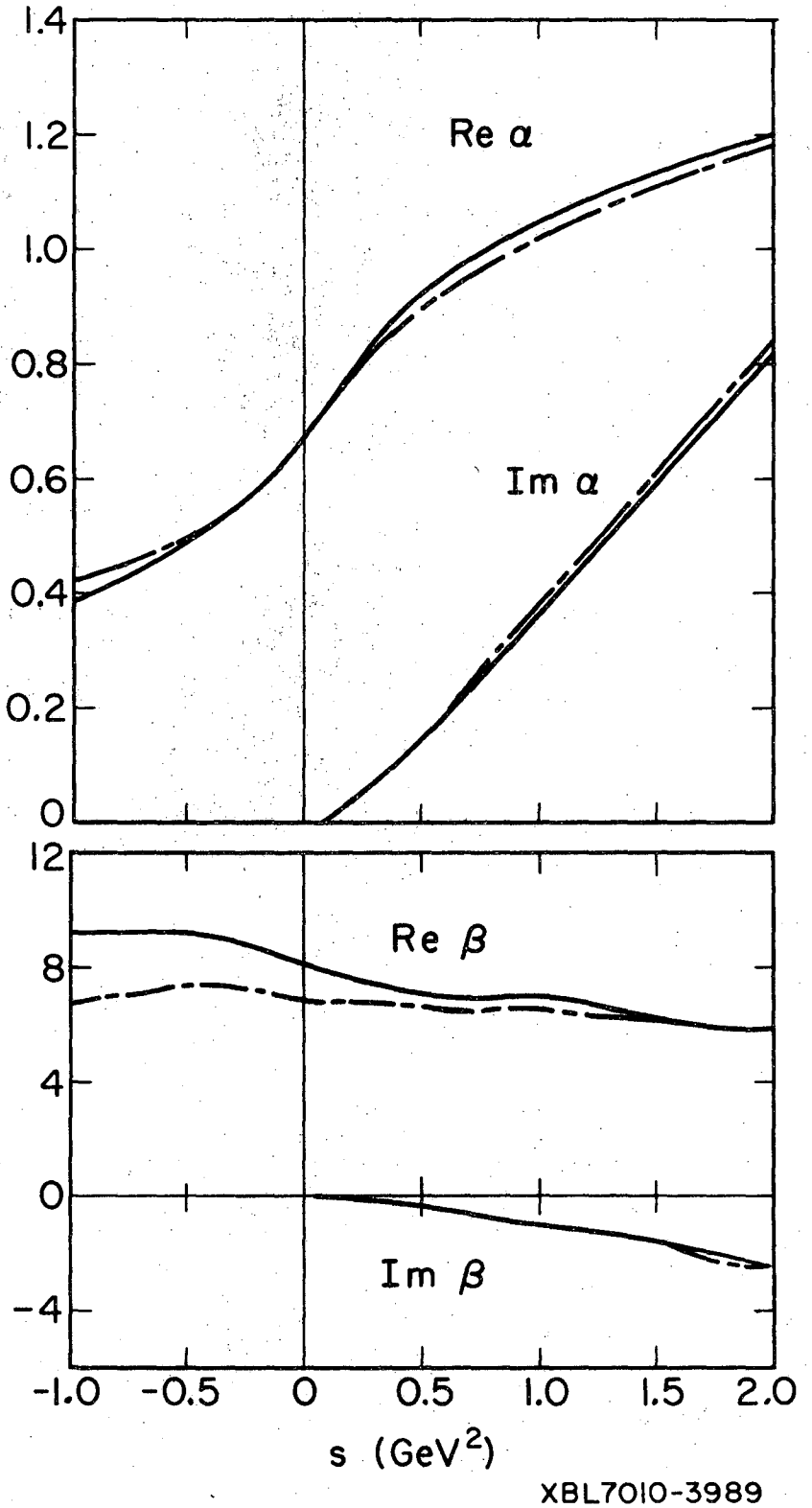
1.4
1.2
1.0
0.8
0.6
0.4
0.2
0
Re α
Im α
12
8
4
0
-4
Re β
Im β
-1.0
-0.5
0
0.5
1.0
1.5
2.0
s (GeV²)
XBL7010-3989

Fig. 7

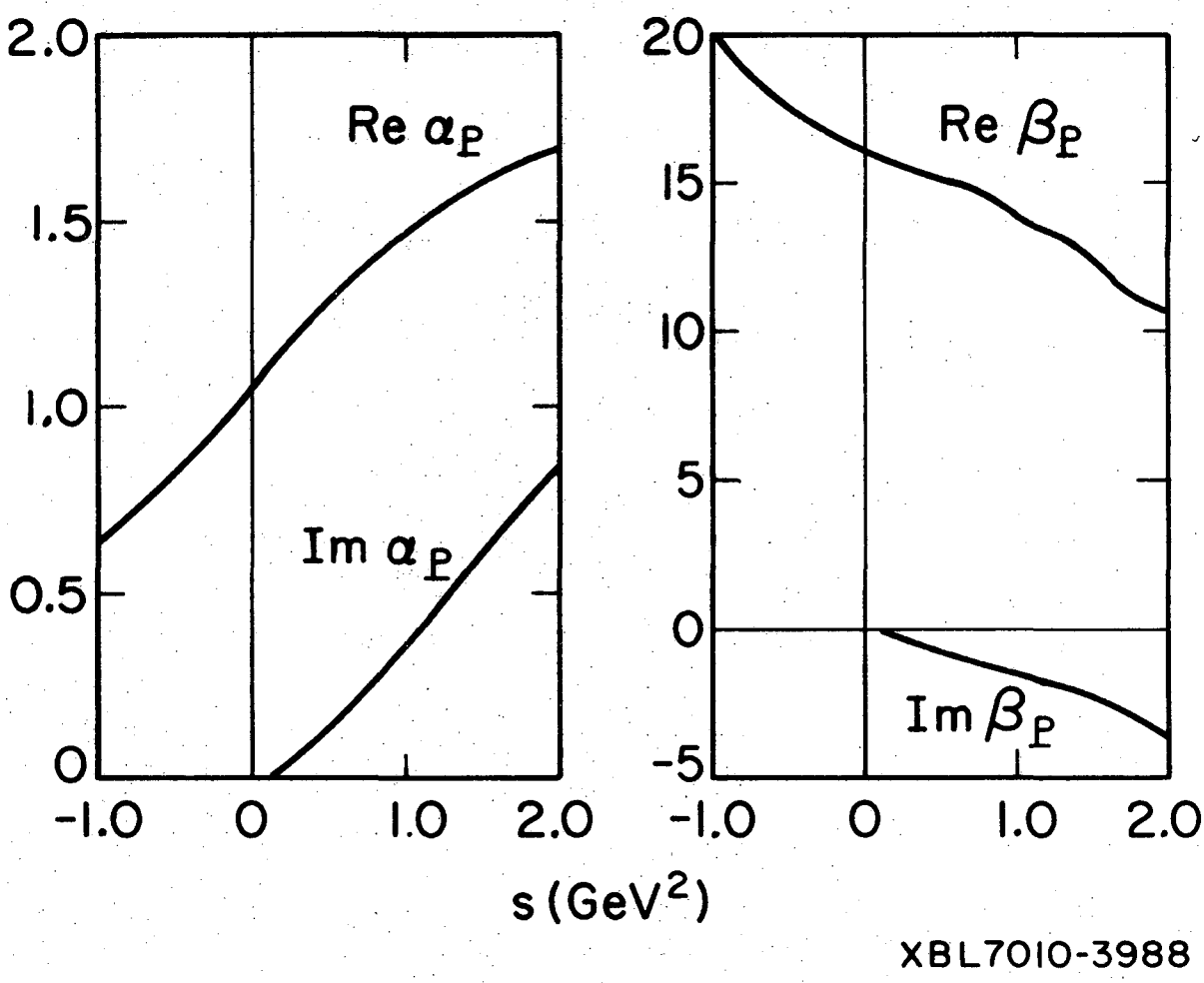
2.0
1.5
1.0
0.5
0
Re α_P
Im α_P
-1.0
0
1.0
2.0
20
15
10
5
0
-5
Re β_P
Im β_P
-1.0
0
1.0
2.0
s (GeV^2)
XBL7010-3988

Fig. 8

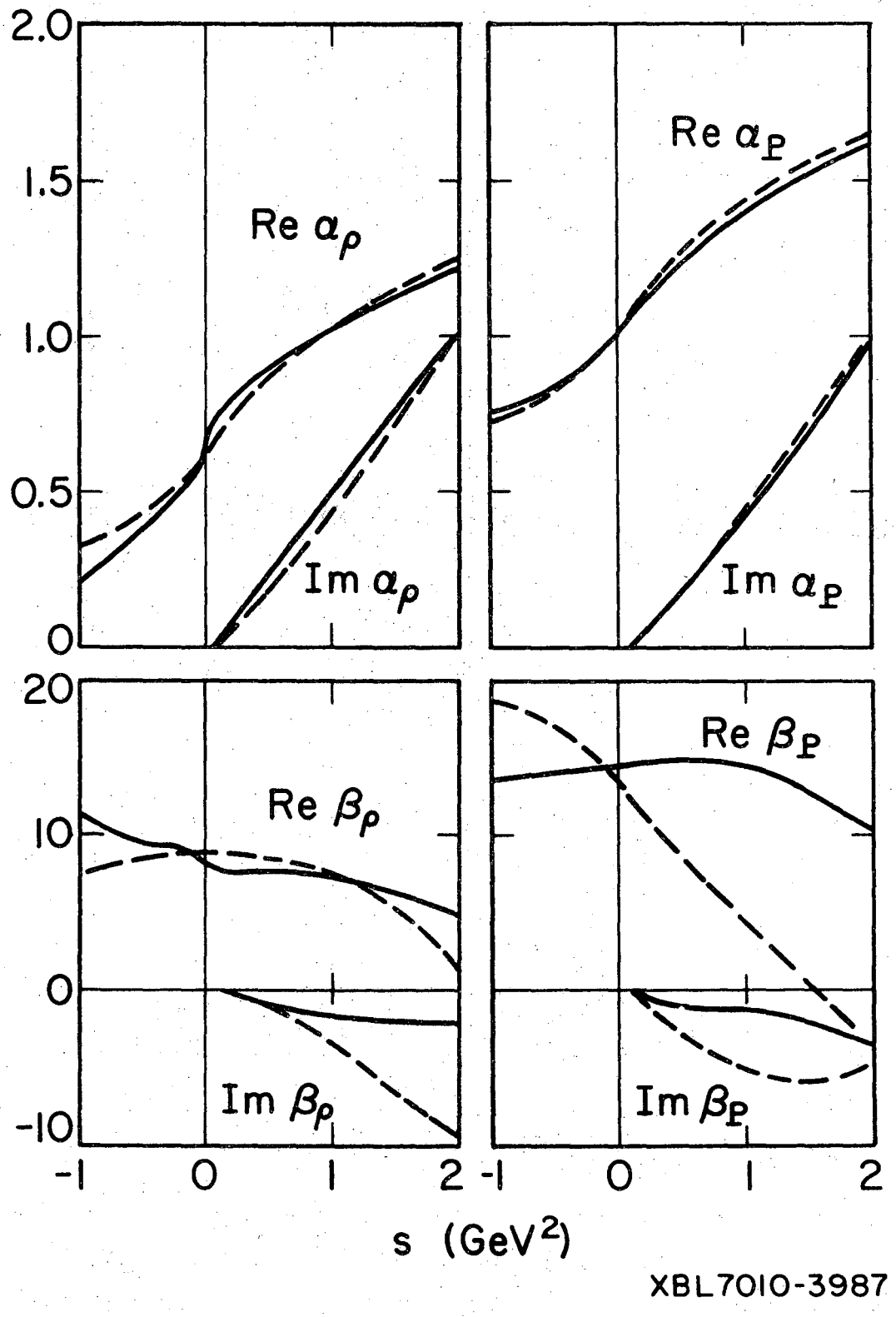
2.0
1.5
1.0
0.5
0
Re α_ρ
Im α_ρ
Re α_P
Im α_P
20
10
0
-10
Re β_ρ
Im β_ρ
Re β_P
Im β_P
-1
0
1
2
s (GeV^2)
XBL7010-3987

Fig. 9

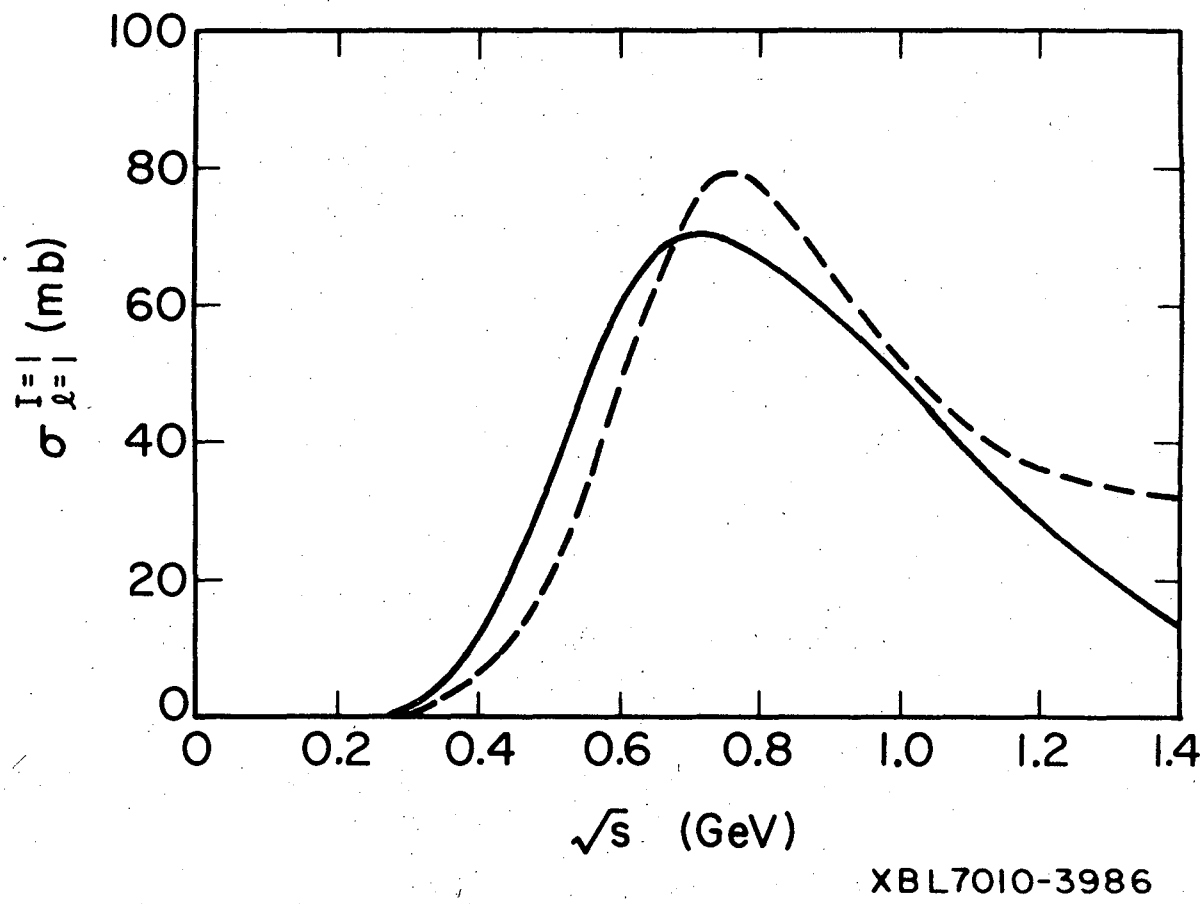
100
80
60
40
20
0
0
0.2
0.4
0.6
0.8
1.0
1.2
1.4
$\sigma_{\ell=1}^{I=1}$ (mb)
$\sqrt{s}$ (GeV)
XBL7010-3986

Fig. 10

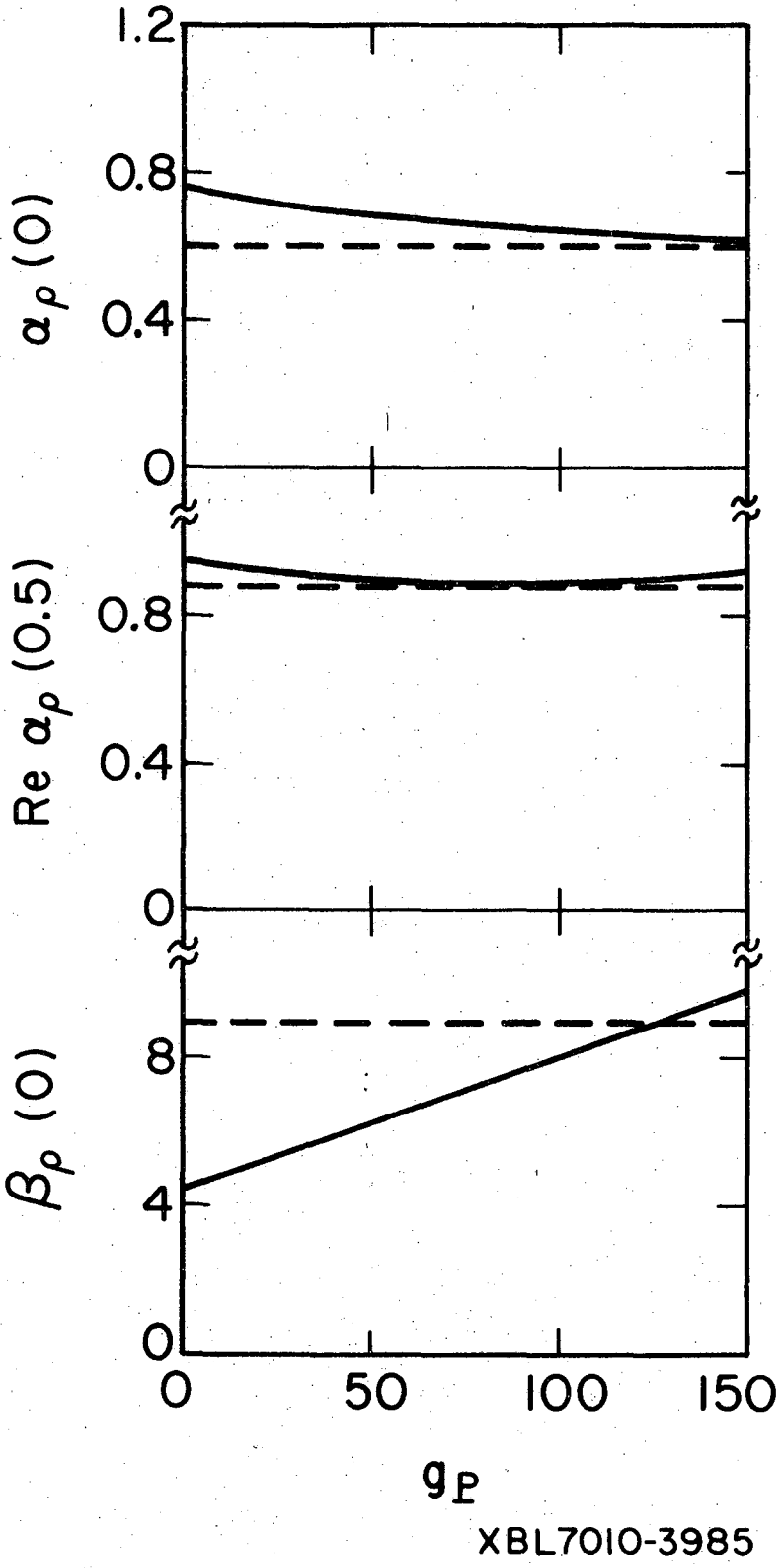
1.2
0.8
0.4
0
α_ρ (0)
0.8
0.4
0
Re α_ρ (0.5)
8
4
0
β_ρ (0)
0
50
100
150
g_P
XBL7010-3985

Fig. 11

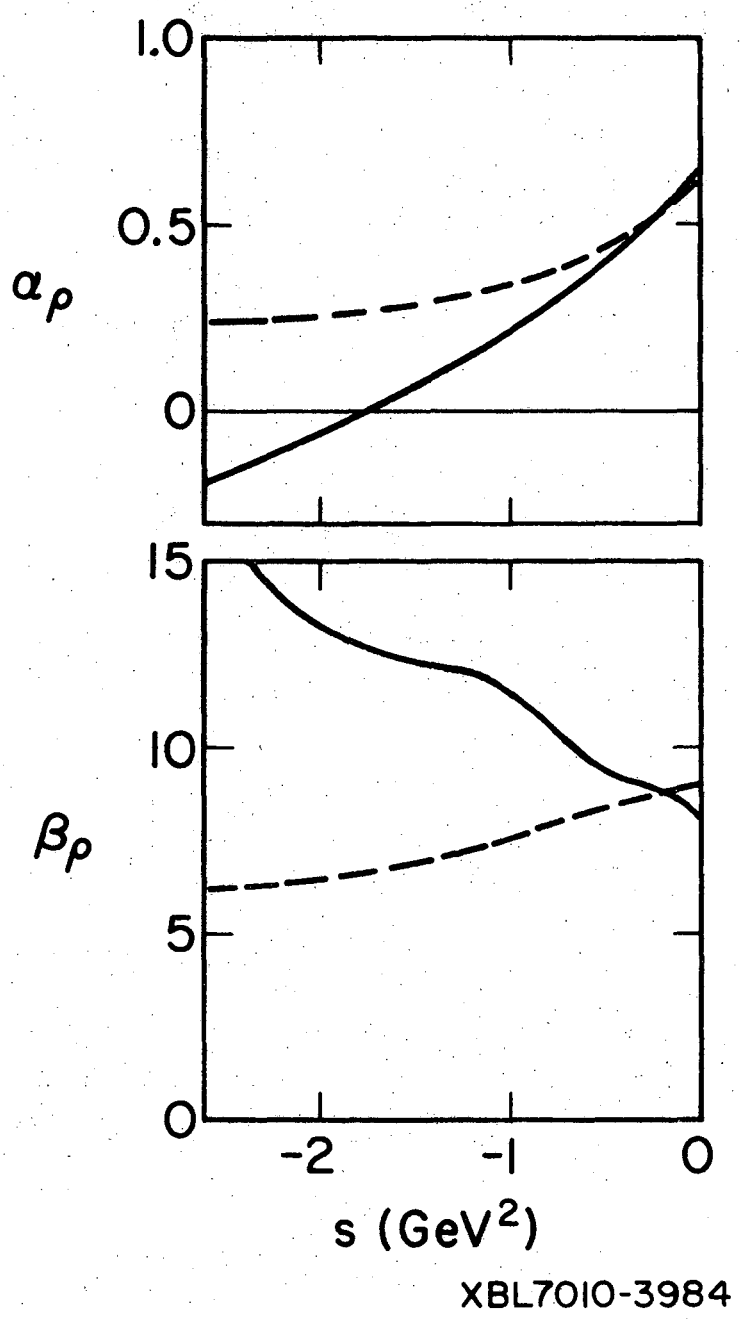

Fig. 12

TECHNICAL INFORMATION DIVISION
LAWRENCE RADIATION LABORATORY
UNIVERSITY OF CALIFORNIA
BERKELEY, CALIFORNIA 94720